Host/Guest Interactions in a Sepiolite–Based Maya Blue Pigment: A Spectroscopic Study

ARTICLE *in* THE JOURNAL OF PHYSICAL CHEMISTRY C · AUGUST 2011

Impact Factor: 4.77 · DOI: 10.1021/jp203270c

7 AUTHORS, INCLUDING:

Kalaivani Seenivasan
Stella Maris College
12 PUBLICATIONS **133** CITATIONS
SEE PROFILE

Gabriele Ricchiardi
Università degli Studi di Torino
89 PUBLICATIONS **4,315** CITATIONS
SEE PROFILE

Michele R Chierotti
Università degli Studi di Torino
72 PUBLICATIONS **1,197** CITATIONS
SEE PROFILE

Roberto Gobetto
Università degli Studi di Torino
298 PUBLICATIONS **4,519** CITATIONS
SEE PROFILE

THE JOURNAL OF PHYSICAL CHEMISTRY C

ARTICLE

pubs.acs.org/JPCC

Host/Guest Interactions in a Sepiolite-Based Maya Blue Pigment: A Spectroscopic Study

Roberto Giustetto,*[,†,§] Kalaivani Seenivasan,[‡,§] Francesca Bonino,[‡,§] Gabriele Ricchiardi,[‡,§] Silvia Bordiga,[‡,§] Michele R. Chierotti,[‡,§] and Roberto Gobetto[‡]

[†]Department of Mineralogical and Petrologic Sciences, Università di Torino, Via Valperga Caluso 35, 10125 Torino, Italy

[‡]Department of Inorganic, Physical and Materials Chemistry, Università di Torino, via Giuria 7, 10125 Torino, Italy

[§]NIS Centre of Excellence, Via Quarello 11, 10135 Torino, Italy

ABSTRACT: Maya Blue pigment forms through heating-induced encapsulation and bonding of indigo in microporous clays, namely, palygorskite or sepiolite. Stabilizing host/guest interactions in a sepiolite-based Maya Blue were investigated by means of vibrational and NMR spectroscopies and proved to be H-bonds formed between indigo reactive groups and the clay structural OH_2. Indigo sorption inhibits sepiolite structural folding induced by partial OH_2 loss with temperature rise, but despite this, no direct Mg/indigo bonding was detected. Encapsulation is favored by breaking of intermolecular bonds, allowing dye diffusion inside the clay microtunnels. H-bond formation involves both C═O/N−H indigo groups, its molecule undergoing distortion and partial oxidation to dehydroindigo. Both the strength and number of sepiolite/indigo interactions are less marked than those occurring in a palygorskite-based composite. In the wider sepiolite channels, H-bonds can form only on one side of the guest molecule, whereas both sides are involved in palygorskite. Halving in bond number undermines the stability of the resulting adduct.

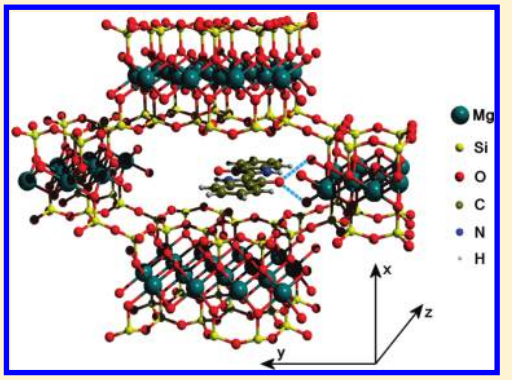

1. INTRODUCTION

Maya Blue is a well-known blue pigment used by ancient Mayas mainly in the Yucatan peninsula (Mexico) from VI to XVI century A.D., to decorate statues, pottery, and mural paintings. Rediscovered in modern times,[1] Maya Blue immediately catalyzed the interest of the scientific community due to its astounding stability being basically unaffected by both acids and alkali attacks and immune to light exposure.

It is nowadays reckoned that Maya Blue has to be considered a precursor of modern nanocomposite materials, in which the guest indigo dye is adsorbed on a hosting microporous clay (palygorskite and/or sepiolite). Procedure for the pigment preparation is well-known, both using raw materials and ancient Mayan technologies (clays extracted from local outcrops and indigo from the leaves of *Indigofera suffruticosa*[2]) or pristine precursors and laboratory techniques.[3,4] The simplest way to obtain a stable pigment consists in dry grinding the clay (palygorskite or sepiolite) with proper indigo amounts (≤2 wt %) and moderately heating (120−190 °C) for variable times (30 min to several hours). Everlasting stability is achieved during heating as a ground but unheated clay/indigo mixture, although, similar in aspect to Maya Blue, is discoloured when attacked by acids.

Sepiolite is a fibrous colorless clay mineral and an end-member in the palygorskite-sepiolite group. Its structure can be described as a chessboard-like disposition of TOT units,[5] with octahedral (O) sheets broken in ribbons elongated in the [001] direction and tetrahedral (T) sheets, which maintain their continuity thanks to a periodic inversion in the orientation of the apical oxygen atoms, pointing alternatively up and down and bonding to the upper or lower discontinuous O strip (Figure 1a). Microtunnels, filled by weakly bound zeolitic H_2O and exchangeable cations, cross the structure along [001]. Tightly bound, structural OH_2[6] completes the coordination of Mg ions at the edges of the O ribbons.

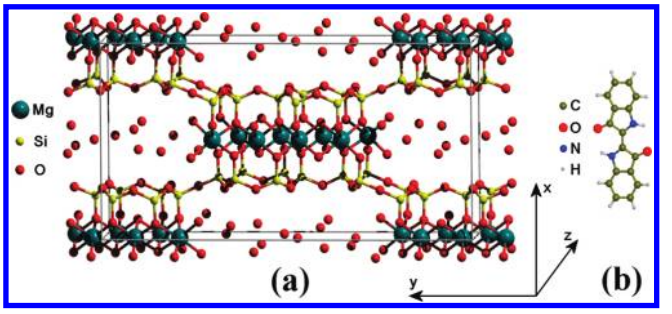

Figure 1. (a) The structure of sepiolite (Post et al.[50]); (b) the indigo molecule.

Differences between sepiolite and palygorskite stand in the tunnel dimensions (10.6 × 3.7 Å in the former and 6.4 × 3.7 Å in the latter), TOT ribbons width (eight O sites in the former and

Received: April 8, 2011
Revised: July 4, 2011
Published: July 22, 2011

five in the latter), and O sheet composition (presence of quasi-exclusive Mg in the former and Mg, Al, and subordinate Fe^{3+} in the latter). Due to their sorption properties, both clays have been studied with regard to their potential applications as adsorbents of small organic molecules[7,8] and dyes[9−11] within the tunnels or on the fiber surface and as support for catalysts.[12−14]

Indigo is a well-known blue dye whose molecule (Figure 1b) contains a cross-conjugated chromophore composed of a central C═C bond carrying two donor (amine units: N−H) and two acceptor groups (carbonyl units: C═O).[15] Distribution of the electric charge in the basic chromophore shows high polarizability and is strongly influenced by intermolecular forces.[16]

The amount of indigo reacting with the clay during Maya Blue synthesis is reputed to be quite low. A complete substitution of all zeolitic H_2O with indigo would imply the presence of a 7.1 dye wt % in sepiolite, although minor quantities are indeed expected to enter the framework tunnels under controlled synthetic conditions (4.0−4.5 wt %).[17] Despite this, an even more limited H_2O substitution is likely to occur while preparing the pigment in the experimental conditions used by the ancient Mayas, thus explaining why the indigo content in original Maya Blue is expected not to exceed 2 wt %.[4,18−21] Though higher quantities have been used in previous experiences,[22−25] the addition of excessive dye amounts appears inadequate as its limited interaction with the activated clay causes the presence of a useless, nonbonded surplus. Additionally, the typical blue color of original Maya Blue is achieved by using the recommended quantity (≤2 wt %), higher amounts resulting in much darker hues. In order to avoid the presence of excess indigo, the freshly synthesized pigment has to be purified with a Soxhlet extractor in proper solvents after preparation.[4,17]

In Maya Blue, indigo is likely to be distributed in different sites in the hosting clay framework,[26] together with other subordinate derivatives (i.e., dehydroindigo - the oxidized form of indigo[23,26−28]). Several spectroscopic techniques have been used so far to investigate the structural features of this nanostructured hybrid material and the sorption of the organic dye in the inorganic framework − especially when palygorskite is the hosting matrix. Additionally, the possible hosting of indigo on alternative porous matrices (i.e., zeolites) has also been considered.[29] The real nature of the host/guest interactions responsible for the Maya Blue stability, however, is still disputed, whether H-bonds between indigo reactive groups (C═O/N−H) and structural OH_2[18−20,30,31] or direct cation-carbonyl bonds[22,32,33] within the channels. Although alternative hypotheses involving superficial interactions have also been proposed,[21,34] it is acknowledged that limited diffusion of the guest dye inside the palygorskite tunnels happens, as only partial rehydration occurs after heating and no perturbation affects the superficial silanols.[35] Furthermore, the nature of the clay/indigo interaction may be strongly influenced by the heating conditions adopted during the pigment synthesis: temperatures between 350 and 550 °C, sometimes used in the literature,[32,33,36] are likely to affect both the reactivity of the clay—increasing the quantity of absorbable guest molecules—and the nature/site of the mutual bonds. It is reputed, however, that the ancient Mayas did not reach such temperatures during Maya Blue preparation, recent outcomes proving that a moderate heating (around 120−150 °C; definitely below 200 °C) is sufficient to form a stable pigment.[2,35,37] Clay/indigo adducts subjected to anomalously intense thermal treatments may therefore be considered, rather than Maya Blue analogues, alternative composites with peculiar structural features useable in a range of possible applications (paints, polymer reinforcements, control release, carriers and optics).[23]

While most papers have focused on the indigo fixation in palygorskite, only a few have dealt with structural characterization when sepiolite is the hosting framework. The guest indigo molecule is supposed to enter the porous clay matrix during heating due to significant H_2O loss,[23,26,34,36] its diffusion being facilitated by the wider sepiolite tunnels (10.6 × 3.7 Å). Sepiolite−indigo composites are known to be less stable than their palygorskite-based analogues, possibly due to a more pronounced fragility of the former clay structure.[37] Encapsulation and bonding to the clay framework, however, is expected to shield the dye molecules from external environment and prevent deterioration. The potential intercalation of different dyes—other than indigo—in the sepiolite framework was also recently studied by means of confocal fluorescence microscopy.[38]

On the basis of these assumptions, the crystal-chemical surroundings of indigo in a sepiolite-based Maya Blue pigment were investigated by means of several spectroscopic techniques (Fourier transform infrared (FTIR), Raman, and solid-state NMR), following an approach seldom adopted in the past by using different experimental conditions[23] and/or reaching only preliminary results.[39] Changes in the ν(OH) and δ(OH) frequencies and in proton chemical shift, in fact, are well-known useful parameters to detect H-bonding of water molecules,[40,41] which are known to play an important role in this and/or analogous composites.[20,23,35] The need for uncontaminated materials made it impossible to analyze original Maya Blue specimens, as the archeological pigment lacks the requested purity. Such samples always include traces of the substratum below (i.e., plaster or mortar) and rarely contain pristine clay minerals. Palygorskite or sepiolite are predominant and often mixed, although other lamellar clays (such as Illite, montmorillonite and vermiculite) may be present too. Pure sepiolite-based Maya Blue specimens are extremely rare. The current study was therefore performed on freshly synthesized sepiolite + indigo adducts, as already done in previous works.[18,19,34]

In order for the sepiolite−indigo composite to possibly be consistent with both procedures and materials handled by ancient Mayas, 2 wt % indigo was used to prepare the pigment, and the heating temperatures were kept below 200 °C.

2. EXPERIMENTAL METHODS

Natural sepiolite and synthetic indigo were provided by Sigma-Aldrich (cod. nos. 70253 and 56980, respectively). Preparation of Maya Blue analogues followed the well-established procedure codified in the literature.[3,4,22,37] Sepiolite was mixed and dry ground with synthetic indigo (2 wt.%), dispersed in a Petri dish with deionized H_2O and heated up to 190 °C for 22 h. The resulting blue powder was Soxhlet extracted in $CHCl_3$ for 12 h, until no further color loss was observed.

A different procedure was adopted to prepare some of the specimens studied by means of infrared (IR) spectroscopy. Sepiolite was preliminarily activated in vacuum at room temperature, 120°, and 150 °C for 1.5 h in order to progressively (and reversibly) remove the zeolitic H_2O. The activated clay was manipulated in a glovebox (in Argon atmosphere) and ground with 2 wt % indigo. Such mixture was used to make a pellet that was inserted in an IR cell inside the glovebox. After Argon removal, the sample was further heated in a vacuum (pressure below 5×10^{-4} mbar) at 120 and 150 °C. IR absorption spectra were collected at each step, under controlled atmosphere, on a FTIR Bruker Vector 70, with a resolution of 2 cm^{-1} and collecting 64 scans for each spectrum.

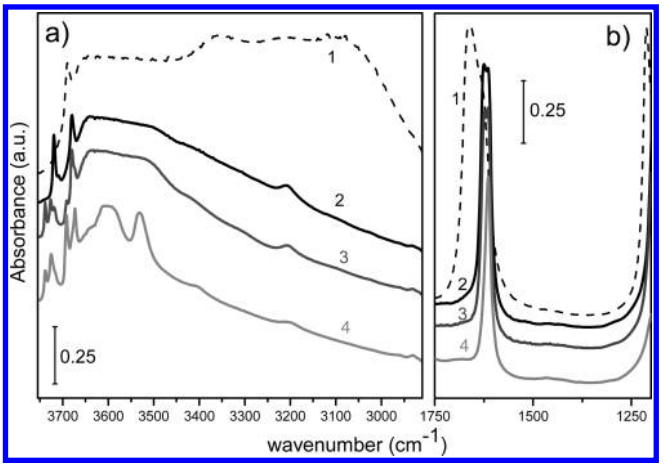

Figure 2. IR spectra of sepiolite in air (1) and evacuated at room temperature (2), 120 °C (3), and 150 °C (4). (a) Hydroxyl stretching region; (b) Hydroxyl bending region.

Raman spectra were collected on powder samples on a Renishaw in Via Raman Microscope with a He−Cd laser emitting at 325 nm. Photons scattered by the sample were dispersed by a 3600 lines/mm grating monochromator and simultaneously collected on a charge-coupled device (CCD) camera; the collection optic was set at the 15× objective. The spectra collection setup of 75 acquisitions, each of them taking 50 s, was adopted.

Solid-state NMR spectra were acquired on a Bruker Avance II 400 spectrometer operating at 400.23 and 100.64 MHz for the ^{1}H and ^{13}C, respectively. For ^{1}H MAS measurements, powdered samples were spun at 32 kHz at room temperature in a 2.5 mm zirconia rotor, using the DEPTH sequence ($\pi/2-\pi-\pi$) for suppressing the probe background signal. A 90° pulse duration of 1.95 μs and 16 transients were collected for each spectrum with a pulse delay of 5 s. ^{13}C cross-polarization magic angle spinning (CPMAS) spectra were recorded using a 4 mm probe at a spinning speed of 12 kHz. A standard ramp cross-polarization pulse sequence was used with a contact time of 3.5 ms, a ^{1}H 90° pulse of 2.95 μs, a recycle delay of 10 s, and a number of transients of 30 000.

Proton and carbon chemical shift were externally referenced via the resonance of polydimethylsiloxane (PDMSO) (^{1}H at 0.14 ppm) and glycine (^{13}C CH_2 signal at 43.86 ppm relative to tetramethylsilane (TMS)).

3. RESULTS AND DISCUSSION

3.1. FTIR Spectroscopy. In order to follow the evolution of the composite IR-active modes during the pigment preparation, FTIR data were collected while progressively heating in vacuum a preactivated sepiolite specimen mixed and ground with a 2 wt % indigo content. Such a procedure allowed us to eliminate the contribution of broad signals related to weakly bound zeolitic H_2O, in order to better appreciate the variations of IR maxima involved in the establishment of host/guest interactions.

Conventional FTIR data were also collected in air on an untreated, freshly synthesized sepiolite-based Maya Blue specimen (hydrated), prepared according to the traditional procedure and Soxhlet extracted in $CHCl_3$ (see paragraph 2), in order to possibly evaluate analogies and/or differences with respect to the IR patterns collected during the synthesis under controlled environmental conditions.

3.1.1. Sepiolite. Collected spectra are consistent with literature data, although different experimental parameters or slight changes in chemical composition may influence the data quality.[42−44]

For the sake of simplicity, spectroscopic features related to stretching modes (Figure 2a) will be described first with respect to those related to bending modes (Figure 2b). Sepiolite in air at room temperature contains both physisorbed and zeolitic H_2O, whose broad signals tend to hide the less intense, narrower bands related to hydroxyls engaged in stronger interactions (Si−OH and Mg−OH_2 bonds). This causes the spectrum stretching region (dashed curve 1 in Figure 2a) to be relatively featureless, with a sharp peak at 3690 and a broader band at 3355 cm^{-1}, related to ν(OH) in the octahedral layer[45] and in zeolitic H_2O,[43] respectively. Once sepiolite is dehydrated in a vacuum at increasing temperatures (room temperature to 120 °C to 150 °C), weakly bound physisorbed, zeolitic H_2O and possibly a fraction of structural OH_2 are lost in different sequential steps. Disappearance of the related broad signals allows progressive detection of the vibrational modes related to tighter-bound hydroxyls.

Most significant spectral changes with temperature rise in the OH stretching region (Figure 2a) consist of the following: (i) Nearly total erosion of the intense broad band extending until around 3000 cm^{-1} (dominant in curve 1) due to physisorbed and zeolitic H_2O (dashed curve 1). (ii) A narrow band appearing at 3720 cm^{-1} (curve 2) when the sample is evacuated at room temperature, related to the Si−OH stretch,[23,43,46] slightly shifts toward higher frequencies (3726 cm^{-1}) after heating at 120 and 150 °C (curves 3 and 4, respectively). In addition, a new feature (fundamental OH stretch[46]) appears at 3738 cm^{-1} forming a close doublet with the previous one. Such variations account both for perturbation of sepiolite silanols with increasing temperature (as observed also for some zeolites[47]) and for liberation of the Si−OH group located at the edge of the O ribbons after folding of the structure due to loss of the first structural OH_2 fraction.[48] (iii) The above-mentioned 3690 cm^{-1} maximum (curve 1, dashed) slightly red-shifts in vacuum at 3680 cm^{-1}, in agreement with the intense fundamental OH stretch reported by Cannings.[46] Temperature rise (120−150 °C) causes further red-shift to 3673 cm^{-1} and the appearance of a new feature at 3691 cm^{-1}, forming a doublet with the previous one. Splitting accounts for perturbation of hydroxyls in the octahedral sheet (Mg−OH): in fact, as loss of the first half of structural OH_2 and transformation to sepiolite dihydrated occurs,[23,45] the consequent structural folding causes the remaining OH_2 molecule to exert a H−H repulsion with the octahedral framework hydroxyls.[48] (iv) In the 3650−3400 cm^{-1} region no appreciable change is observed until 150 °C (possibly due to presence of residual zeolitic H_2O), when two broad bands appear at 3600 cm^{-1} (possible shoulder at 3638 cm^{-1}) and 3531 cm^{-1}, respectively (curve 4), corresponding to Mg-coordinated OH_2.[23,44−46]

According to literature data, loss of tightly bound OH_2 occurs in two steps, beginning at 280−320 °C in air[49,48] and progressively continuing over a wide range of temperatures before completion (first half at 377 °C and second half at 627 °C[36]). Dehydroxylation with transformation to an amorphous phase occurs at higher temperatures (≥800 °C[50,51]). It is well-known that structural folding of sepiolite is induced by the loss of the first half of Mg-coordinated OH_2 and implies rotation of the clay structure about axes parallel to the tunnel elongations (i.e., z crystallographic axis),

which cross the Si−O−Si bonds located on the edges of the TOT ribbons.[52,48−50] While the average sepiolite structure at room T (full OH_2 content) can be considered a tetrahydrated phase, such a transformation causes a sensible reduction in the channel width with passage to a dihydrated phase (SEP4H_2O vs SEP2H_2O, respectively, according to Ovarlez et al.[53]). Previous experiences proved that appearance of dihydrated sepiolite is likely to happen at even lower temperatures in vacuum: under such conditions, loss of the first half of structural OH_2 is due to begin around 120 °C and be complete between 175 and 200 °C.[48] At the adopted extreme experimental conditions (150 °C in vacuum), it is therefore legitimate to repute that a relevant fraction of the first half of structural OH_2 has already left the structure; such an assumption is corroborated by the analogies existing between our spectra and others proposed in the literature for which the same shift of the Si−OH feature (from 3720 to 3738 cm^{-1}) and splitting of the Mg−OH related maximum (from 3680 to 3673 and 3691 cm^{-1}) were described and attributed to folding of the sepiolite structure.[44,48] The presence of two broad maxima at 3600 and at 3531 cm^{-1} (curve 4 in Figure 2a, assigned to OH_2 antisymmetric and symmetric stretching frequencies respectively), however, ensure that most structural OH_2 is still present in the clay structure. Post et al.,[50] while progressively heating in air proved that loss of the first half of the structural OH_2 (and consequent structural folding with transformation to dihydrated sepiolite) is likely to cover a 50 °C interval, starting at 327 °C and ending at 377 °C, thus individuating a feasible temperature range in which both tetra- and dihydrated sepiolite may coexist in the same sample. The same situation is expected to happen in vacuum in an analogous temperature interval, although shifted at lower temperatures. As the adopted extreme experimental conditions (150 °C in vacuum) are slightly below the values expected to ensure complete loss of the first structural OH_2 (175 °C in vacuum[48]), folding of the structure with transformation to dihydrated sepiolite may not be complete in the analyzed specimen, some portions still conserving their tetrahydrated arrangement with unfolded channels. Further heating at higher temperatures (i.e., 530 °C in vacuum or over 600 C° in air; not shown), however, causes OH_2 related bands (3600 and at 3531 cm^{-1}) to disappear due to irreversible loss and formation of sepiolite anhydride.[44−46,49,48]

Figure 2b shows the corresponding IR spectra in the range of hydroxyl bending modes. When collected in air at room temperature (dashed curve 1), a major broad feature appears at 1660 cm^{-1} (shoulder at 1629 cm^{-1}) related to both physisorbed/zeolitic H_2O and Mg-coordinated OH_2.[43,45] Slight shifts in position with respect to literature data might depend on the strength of mutual H-bonds existing between OH_2 and H_2O[43,54−56] as well as different molecular environments resulting from crystal−chemical compositions.[57] These maxima are fundamental to study the OH bending in sepiolite, as they appear in a region clear from other modes.[43,58] On the edge of out-of-scale modes related to the Si−O stretch[43] (below 1200 cm^{-1}), a component is observed, although the high intensity of the spectra makes it impossible to assign a clear maximum.

Dehydration in vacuum at increasing temperatures implies variations that can be resumed as follows: (i) Evacuation at room temperature erodes the component associated with physisorbed water as the growth of a complex band centered around 1620 cm^{-1} is observed. The very high intensity does not allow sharp identification of the maxima positions. Successive heating implies a progressive intensity decrease until at 150 °C a sharp, symmetric band is observed at 1616 cm^{-1}, as expected for

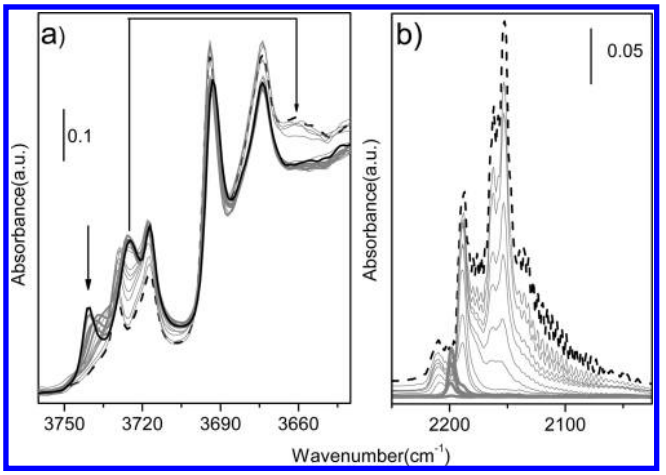

Figure 3. IR spectrum of sepiolite outgassed at 150 °C (black curve), effect of increasing CO dosages (gray curves), and the spectrum obtained at the highest coverage (dashed black curve). (a) Hydroxyl stretching region; (b) CO stretching region. Spectra are reported after sepiolite background subtraction.

δ(OH) of structural OH_2. The observed intensity decrease is consistent with the alleged loss of a relevant fraction of the first half of structural OH_2,[48] implying folding—although incomplete—of the sepiolite structure occurred with possible coexistence, in the analyzed specimen, of both di- and tetrahydrated sepiolite. (ii) A component emerging from the framework stretching modes in air (absorption around 1200 cm^{-1}) tends to disappear with progressive heating in vacuum, suggesting that such a feature could be related to the up-warded γ mode of physisorbed H_2O.

In order to probe the potential accessibility and acidity of different hydroxyl groups in the clay structure, IR spectra were collected on a sepiolite specimen—a self-supporting wafer previously activated at 150 °C in vacuum (pressure below 5×10^{-4} mbar)—exposed at progressively increasing dosages of CO adsorption at liquid nitrogen temperature. Such a procedure is known to be a valid approach used extensively for the characterization of microporous materials.[59,60] The related results are reported in Figure 3. The black curve (Figure 3a) illustrates the IR spectrum of the activated sepiolite in the hydroxyl stretching region (attribution of each maximum has been detailed above); upon interaction with increasing CO dosages, the gray set of curves is obtained. The dashed curve (Figure 3a) appears as the result of CO maximum coverage (20 mbar equilibrium pressure of CO) at the liquid nitrogen temperature.

As expected, most sepiolite OH groups show no significant perturbation upon CO adsorption. Framework hydroxyls co ordinated to Mg cations evidence no particular interaction as the related IR maxima (3693 and 3673 cm^{-1}) remain basically unaltered in spite of progressively increasing CO dosages (Figure 3a). The band at 3741 cm^{-1}, on the contrary, gradually shifts at lower frequencies, mixing with bands below 3660 cm^{-1}, while the component at 3725 cm^{-1} shifts at 3662 cm^{-1} (see arrows in Figure 3a). These significant movements toward lower wavenumbers imply a moderate perturbation of the superficial silanols may happen consequent to CO adsorption.

Figure 3b shows the corresponding situation in the ν(CO) counterpart region. Overall weak intensities of the related bands suggest that CO adsorption in sepiolite is generally modest.

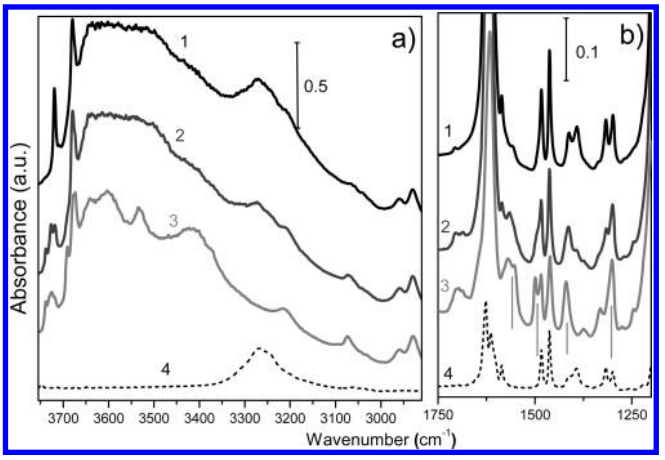

Figure 4. IR spectra in the OH stretching (a) and bending (b) regions of preactivated (120 °C) sepiolite + indigo (2 wt %) adduct evacuated at room temperature (1), 120 °C (2), and 150 °C (3). IR spectrum of synthetic indigo is reported as a dashed curve (4) for comparison.

However, the appearance of a complex multiplet (maxima at 2210, 2200, 2188, 2165, 2153, and 2138 cm^{-1}) indicates that a variety of possible framework sites are involved. Among these, features appearing at 2138, 2153, and 2165 cm^{-1} can easily be attributed to CO physisorption on the clay surface and to CO interacting with two slightly different superficial silanol groups, respectively. Components at 2188, 2200, and 2210 cm^{-1}, on the other hand, can only be explained by considering the possible effect of strong polarizing centers acting as Lewis sites. The higher frequency values observed for CO could therefore be explained by limited adsorption operated by few Al and/or Mg species located in defects such as external surfaces, although alternative locations (i.e., inside the clay channels) can also be considered. A direct interaction between CO and Al/Mg ions cannot therefore be excluded at the adopted experimental conditions.

3.1.2. Sepiolite + Indigo (2 wt %) Adduct. The IR spectrum of synthetic indigo (Figure 4a,b, dashed curve 4 at the bottom) proved to be consistent with those published in the literature, with its main features lying in the 1000−1650 cm^{-1} region (attributions according to Tatsch and Schrader[15]). Most significant vibrational modes are the antisymmetric ν(C═O), forming a doublet at 1626 and 1614 cm^{-1}, and the in-plane δ(N−H), forming another couple at 1412 cm^{-1} (shoulder, intramolecular N−H/C═O bonds) and 1393 cm^{-1} (intermolecular bonds). In pristine indigo, these bonds are responsible for the linkage of different molecules in trans-form.[36,61−63] Broad ν(N−H) appears at 3268 cm^{-1}.

Addition of indigo to sepiolite and progressive heating modify the spectral features of both isolated precursors. In spite of its low amount (2 wt %), indigo bands are easily identifiable in the composite spectra, and the absorption maxima of the hosting matrix, particularly those related to H_2O and OH_2, modify their positions and intensities.

The hydroxyl stretching region (2900−3750 cm^{-1}) of an activated sepiolite + indigo (2 wt %) mixture heated in vacuum at progressively increasing temperatures is shown in Figure 4a.

When crushed in vacuum at room temperature (curve 1 in Figure 4a), the spectrum is quite similar to that of pristine sepiolite with the exception of a broad feature appearing at 3270 cm^{-1}. Such a band corresponds to ν(N−H) of indigo, basically unperturbed with respect to the pristine dye (curve 4 in Figure 4a). The lack of any related shifting indicates that host/guest interactions are not established yet.

Heating in vacuum at 120 °C has no dramatic effect on the IR pattern (curve 2 in Figure 4a), although the intensity of the ν(N−H) maximum slightly decreases and red-shifts (shoulder at 3212 cm^{-1}), suggesting that interactions with the sepiolite matrix start to form. Other variations in the 3800−3400 cm^{-1} range are consistent with those observed for sepiolite: silanol perturbation (splitting of the 3720 cm^{-1} band) is not altered by the presence of indigo, implying no superficial clay/dye interactions occur. The appearance of a band at 3072 cm^{-1}, absent in sepiolite, is due to the ν(C−H) of indigo.

Further heating at 150 °C (curve 3 in Figure 4a) involves the following effects: (i) Surface silanols (band at 3725 and shoulder at 3738 cm^{-1}) show no appreciable variation, thus excluding the possibility of a superficial clay/dye interaction and indicating that partial loss of the first half of the sepiolite Mg-coordinated OH_2 is not prevented by the presence of indigo, in agreement with previous thermogravimetric data.[53] (ii) The 3674 cm^{-1} maximum (hydroxyls of the octahedral sheet: Mg−OH) is still evident, whereas the 3691 cm^{-1} band decreases and probably shifts at lower frequency (broader 3640 cm^{-1} feature). Such evidence suggests that indigo fixation is likely to occur inside the hosting clay tunnels, where it allegedly inhibits structural folding of sepiolite in spite of the intervened loss of a significant fraction (nearly half) of structural OH_2. The presence of indigo, therefore, causes the structure of dihydrated sepiolite not to collapse, which is consistent with evidence described by previous authors.[23,53] (iii) Maxima at 3600 and 3531 cm^{-1} are basically left unchanged with respect to pristine sepiolite, implying that at least half of the Mg-coordinated OH_2 is still in the channel in spite of the applied heating. A broad and completely new band, however, appears at lower wavenumbers (3420 cm^{-1}), finding no counterpart in pure sepiolite or indigo IR spectra. The most feasible explanation is that such broad feature accounts for a perturbed fraction of coordinated OH_2 involved in H-bonds with the guest indigo molecules. Such interactions, albeit usually considered weak, when formed within narrow surroundings such as the sepiolite tunnels, are hardly reachable and therefore tough to break. (iv) The band related to indigo ν(N−H) definitely red-shifts, peaking at 3212 cm^{-1}, accounting for completion of the newly formed host/guest interactions. The observed shift (−55 cm^{-1}), although slightly higher than the theoretical one calculated with ab initio quantum methods (−38 cm^{-1}),[20] is consistent for an indigo molecule involved in interaction with H_2O. (v) The fundamental role of indigo in the strengthening of host/guest interactions is further justified by the increase in intensity of the dye-related feature at 3072 cm^{-1}.

As far as the indigo molecule is concerned, the spectral region reported in Figure 4.b (hydroxyls bending) is even more appealing. As already observed in the high frequency portion, when the composite is evacuated at room temperature (curve 1 and 2 in Figure 4b) the pattern results in an approximate sum of the spectroscopic features of the two isolated precursors. Progressive temperature rise (120 and 150 °C, curves 2 and 3 in Figure 4b, respectively) causes simplification and peaking of the structural OH_2 bending mode at 1615 cm^{-1} (as already observed in pristine sepiolite), together with an intensity decrease, which certifies the intervened loss of a relevant fraction of OH_2 (almost half). Additionally, the appearance on the very same band at 150 °C of a weak additional shoulder at 1640 cm^{-1} can be

observed (curve 3 in Figure 4b). As no similar feature is observed in pure activated sepiolite, such a feeble signal has to be associated with interactions between the hosting matrix and the guest dye, namely, the upward δ mode of structural OH_2 (+ 25 cm^{-1}) involved in H-bonding formation with the reactive groups of indigo (C═O and/or N−H). The modest intensity of this shoulder suggests that the number of species involved in this kind of interaction is small. Similar features can be observed, although more intense, when palygorskite instead of sepiolite acts as the hosting framework of even minor indigo quantities (1 wt %).[20]

As remarked in previous studies,[4,23,36,64] the presence of indigo is also evidenced by the direct appearance of the related modes in the 1600−1150 cm^{-1} region. While in the spectrum of the evacuated mixture at room temperature (curve 1 in Figure 4b) both positions and intensities for indigo bands are consistent with those of the pristine dye (curve 4), gradual heating causes variations due to progressive formation and strengthening of the clay/dye interactions. Most significant changes with temperature rise can be explained as follows: (i) The band related to indigo intermolecular bonding [in-plane δ(N−H): 1393 cm^{-1}] radically decreases in intensity at 120 °C (curve 2) and completely disappears at 150 °C (curve 3 in Figure 4b). Such evolution implies folding of crystalline indigo, whose dissociation to single monomers facilitates diffusion inside the channels.[23,36,64] Breaking of intermolecular bonds, in addition, activates indigo reactive groups (N−H/C═O) rendering them free to interact with the hosting framework. No modification was observed for intramolecular bonds, in spite of a slight shift at 150 °C toward higher wavenumbers of the related feature (from 1412 to1420 cm^{-1}). The persistence of such bonds is consistent with the moderate applied heating, higher temperatures (≥300 °C in air) usually being required for them to split. On the basis of these premises, application of more radical heating treatments (>300 °C) might cause contextual breaking of intramolecular bonds and loss of structural OH_2 (with complete phase transformation to dihydrated sepiolite), thus favoring the formation of direct C═O−Mg bonds whose existence was reported in previous papers.[36,53] (ii) Several bands related to the ν(C−C) of the dye benzene rings significantly vary while heating (main ones underlined by gray vertical bars in Figure 4b): a feature at 1586 cm^{-1} disappears as new components grow at 1569 and 1552 cm^{-1}; a band at 1483 cm^{-1} splits into two separate maxima, with a new feature appearing at 1500 cm^{-1}; the maximum at 1317 cm^{-1} disappears as a new weak band appears at 1332 cm^{-1}. All these variations suggest that the dye molecule may undergo deformations as a result of encapsulation in the hosting matrix. (iii) Weak new maxima appear at 1700 and 1374 cm^{-1} and increase with heating; as no similar features are observed in pure sepiolite nor indigo, they have to be related to their mutual interaction. Similar bands, although slightly shifted, were previously described for similar sepiolite/indigo adducts prepared under different experimental conditions (heated at 300 °C and loaded with up to 11.5 wt % of indigo) and attributed to thermal decomposition of the dye to dehydroindigo.[23] This is consistent with a slight color change of the pigment (from deep- to greenish-blue) noticeable before and after heating. The presence of dehydroindigo is reputed to favor diffusion inside the tunnels.[26,35] (iv) Direct evidence of the involvement of the C═O group in host/guest interactions cannot be ascertained from IR data, as the related antisymmetric feature [ν(C═O): 1626 cm^{-1} in pure indigo] is hidden below the more intense unperturbed $\delta(OH_2)$ band of sepiolite (1615 cm^{-1}). Assignation of the ν(C═O) mode to the above-mentioned 1640 cm^{-1} shoulder lacks consistency, as such an observed potential shift (+14 cm^{-1}) would not agree with the theoretical one calculated with ab initio quantum methods (−3 cm^{-1}).[20]

It is legitimate to assume that evacuation of the sepiolite + indigo (2 wt %) composite at 120 °C, while implying a loss of all zeolitic H_2O, does not affect the hosting clay structural OH_2 content. As a consequence, indigo is likely to be hosted in a fully tetrahydrated matrix, a situation likely to be compared to that existing in archeological Maya Blue.

On the other hand, the extreme experimental conditions adopted while monitoring variations of the IR-active vibrational modes during pigment synthesis (150 °C in vacuum) cause not only the zeolitic H_2O but also a relevant fraction (almost half) of the tightly bound structural OH_2 to leave the sepiolite framework. The presence of indigo, however, prevents structural folding of the hosting framework (lack of the 3691 cm^{-1} IR-active band in the composite patterns), thus causing the appearance of an atypical phase (unfolded dihydrated sepiolite with indigo encapsulated in the channels), whose existence depends on the mutual interactions established between the hosting matrix and the guest molecules. As already observed for pristine sepiolite activated at 150 °C in vacuum, the coexistence of both dihydrated and tetrahydrated portions may occur for the hosting matrix of the clay/indigo composite under the same experimental conditions, as the loss of the first half of structural OH_2 is incomplete. The only feasible difference between these di- and tetrahydrated regions, however, stands in the different levels of hydration of the Mg ions located on the edges of the TOT ribbons —some of them presenting their full OH_2 content, others only half —consequent to the lack of structural folding, which is inhibited by the presence of indigo. The resulting clay/dye adduct, consequently, might provide interactions of the guest dye molecule with both dihydrated and tetrahydrated sepiolite, a situation unlikely to happen in original Maya Blue, where the exclusive presence of the tetrahydrated clay is expected as a consequence of the moderate heating applied during the pigment manufacture (≤200 °C). Such a situation (simultaneous presence of different hydration levels in the hosting framework) is known to affect the nature, extent and strength of the relationships established between the microporous matrix and the guest molecule, involving the possible existence of direct bonding between indigo reactive groups and the Mg ions located on the edges of the TOT ribbons.[65]

As far as the guest indigo vibrational modes are concerned, some selected shifts and intensity variations (shift of the 1412 feature to 1420 cm^{-1}; decrease and shift of the 1317 cm^{-1} band; appearance of a band at 1552 cm^{-1}) observed for the evacuated composite at 150 °C (curve 3 in Figure 4b) indeed coincide with those recently reported for a dihydrated sepiolite + indigo composite heated at 300 °C in air, for which the existence of direct Mg−indigo interactions was reported.[53] In spite of this, no feature—not even weak—can be observed in our patterns in the 2150−2250 cm^{-1} region, where direct evidence related to possible straight interactions between octahedral Mg and the guest reactive groups should be located (see section 3.1.1). As far as the potential instability of the five-coordinated Mg ions in dihydrated sepiolite is concerned,[66] such a situation is likely to be compensated by the renowned reversibility of the semidehydration process.[45,48] This very same phenomenon, in fact, is expected to cause transformation of the unstable alleged direct bonds between Mg and indigo into a different and more stable configuration as time proceeds.[53]

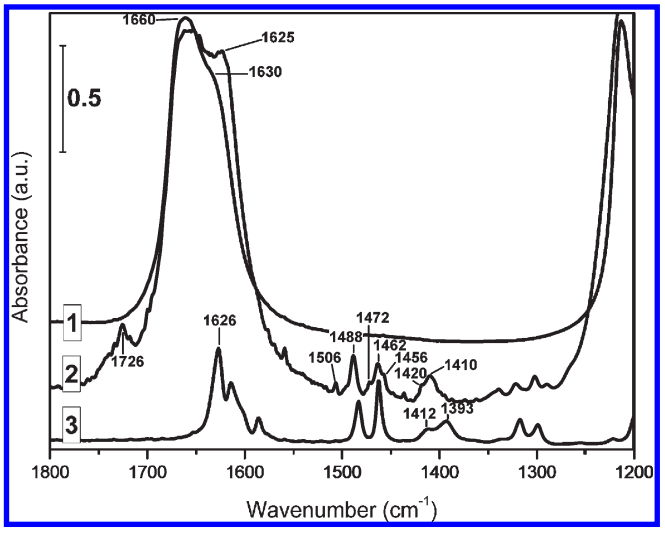

Figure 5. IR spectra in air of pristine sepiolite (1), sepiolite + indigo (2 wt %) adduct after heating and Soxhlet extraction in $CHCl_3$ (2), and pure indigo (3). Spectra are shifted on the Y axis for the sake of clarity.

On the basis of this experimental evidence, the existence of direct interactions between the octahedral Mg and the reactive indigo groups at the adopted extreme experimental conditions (150 °C at pressure below 5×10^{-4} mbar) remains therefore dubious, as all involved shifts and intensity variations related to both the hosting matrix and the guest indigo IR-active modes apparently point to the existence of possible H-bonding interactions with the dye acceptor and donor groups, mediated by sepiolite Mg-coordinated OH_2.

In order to dispose of FTIR data straightly comparable to those collectable on an authentic (archeological) sepiolite-based Maya Blue specimen and consistent with those obtained using other spectroscopic techniques (such as Raman and solid-state NMR, for which freshly synthesized sepiolite-based Maya Blue samples were analyzed, as described below), additional IR data were collected in air at room temperature on pigment specimens prepared according to the conventional laboratory procedure (see Experimental Methods section).

Figure 5 shows the FTIR spectra in air in the hydroxyl bending region (1800−1200 cm^{-1}) of pristine sepiolite (curve 1), indigo (curve 3), and the related host/guest composite obtained after grinding and heating (190 °C in air for 22 h) the clay with the dye (2 wt %) and prolonged Soxhlet extraction in $CHCl_3$ (curve 2). The corresponding stretching interval is not shown, as the presence of broad signals related to weakly bound zeolitic H_2O causes the indigo and coordinated OH_2 IR-maxima to be almost impossible to detect.

The contextual presence of zeolitic H_2O and structural OH_2 in the sample causes the main δ(OH) feature of sepiolite (curve 1) to form a broader signal, peaking at 1660 (shoulder at 1630) cm^{-1}. The addition of indigo (curve 2) apparently causes a new feature to appear at 1625 cm^{-1}, whose position could be consistent with the relevant indigo ν(C═O) appearing at 1626 cm^{-1} (curve 3). Such an attribution, however, is dubious, as all other indigo maxima, when complexed to sepiolite, show significantly lower intensities. An alternative hypothesis may assign this band to the structural OH_2 of the sepiolite tunnels, whose spectral features may be modified by the addition of indigo (curve 2). Broadening of such a band toward higher wavenumbers due to the presence of zeolitic H_2O unfortunately covers up any possible shift of the structural OH_2 bending modes, thus preventing the possibility of appreciating OH_2 involvement in the possible formation of H-bonds with the guest indigo, in opposition to what is described above for the dehydrated sample.

As already mentioned, the 1560−1250 cm^{-1} spectral region of sepiolite shows no significant bands (curve 1), whereas most of the significant IR-active modes of indigo appear in the same interval (curve 3). When the sepiolite + indigo (2 wt %) pattern is concerned (curve 2) several low intensity maxima become visible in that region, thus justifying the dye sorption in the hosting matrix.

Most significant analogies and differences with respect to the evacuated and dehydrated composite IR patterns (Figure 4b) can be summarized as follows: (i) The occurrence of indigo as isolated monomers is confirmed, as intermolecular bonds among molecules tend to break during the pigment synthesis. Such behavior, implying disappearance of the related IR maximum (1393 cm^{-1} band in pristine indigo - curve 3; absent in the composite pattern - curve 2), allows diffusion of indigo inside the sepiolite channels and activation of the related reactive groups (C═O and N−H). The persistence of intramolecular bonds for indigo hosted in sepiolite is also confirmed, although the related maximum (1412 cm^{-1} in pure indigo, curve 3) apparently splits in a doublet centered at 1410 (more intense) and 1420 (shoulder) cm^{-1} (Figure 5, curve 2). The former feature is visible also in the evacuated specimen heated at 120 °C (Figure 4b, curve 2) and shifts toward higher frequency when temperature rises (1420 cm^{-1} at 150°; Figure 4b, curve 3). Scarce intensity of this latter feature in the FTIR pattern collected in air (Figure 5, curve 2) implies that the presence of dihydrated sepiolite, if any, is negligible.[53] (ii) The indigo feature at 1462 cm^{-1} (curve 3), attributed to ν(C−C) and δ(C−H),[15] evidences no significant shift in the clay/dye composite but a moderate intensity decrease, with further appearance of two-sided shoulders at 1456 (more intense) and 1472 cm^{-1} (less intense), respectively. Such splitting, observed neither in the heated/dehydrated composite nor in analogous thermally treated specimens,[23,24,36,53] further supports the theory according to which more or less pronounced deformations affect the indigo molecule after encapsulation within the sepiolite channels. Consistently, most indigo maxima related to benzene rings ν(C−C) show variations that are similar to those described above for the heated/dehydrated specimen: in particular, the splitting of the 1483 cm^{-1} band of pure indigo (Figure 5, curve 3) in a doublet (1488 - more intense; 1506 cm^{-1} - weaker), appearing in the sepiolite-based Maya Blue pattern collected in air (Figure 5, curve 2), is consistent with the analogous behavior observed for the evacuated composite specimen heated at 120 °C (Figure 4b, curve 2). (iii) A new and moderately intense feature appears at 1726 cm^{-1} in the sepiolite + indigo (2 wt %) pattern (Figure 5, curve 2). As already mentioned above, such a band is likely to be related to the mutual clay/dye interaction and specifically to the transformation of indigo to its oxidized form. A similar feature, although slightly shifted, was previously observed on analogous materials[23,24,53] and attributed to the carbonyl frequency of dehydroindigo.[67]

The FTIR pattern collected in air on a freshly synthesized and Soxhlet-extracted (in $CHCl_3$) sepiolite-based Maya Blue specimen therefore shows relevant analogies with the one collected in vacuum on a sepiolite + indigo (2 wt %) composite heated at 120 °C. In both cases, in fact, the guest indigo molecule is expected to interact during the pigment preparation with a sepiolite matrix deprived of zeolitic H_2O but fully hydrated as

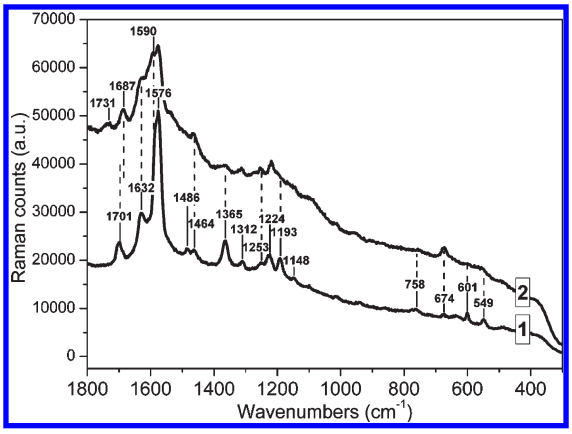

Figure 6. Raman spectra of indigo (1) and sepiolite + indigo (2 wt %) adduct after heating and Soxhlet extraction in $CHCl_3$ (2).

far as the Mg-coordinated OH_2 is concerned: no significant OH_2 loss, in fact, is expected to have occurred or—if any—to have been replaced by rehydration. The applied thermal treatments (heating at 190 °C in air or at 120 °C in vacuum), emptying the clay tunnels from zeolitic H_2O but leaving all OH_2 in situ, favor diffusion of indigo monomeric units but cannot induce formation of (unfolded) dihydrated sepiolite. As a consequence, the nature of the related clay/dye interactions is the same for both situations, being represented by H-bonding interactions between indigo reactive groups and sepiolite Mg-coordinated OH_2.

It appears obvious, on the other hand, that adoption of progressively more severe thermal treatments—both in air (≥300 °C) and in vacuum (≥150 °C)—causes the shifts and intensity variations of the guest indigo vibrational modes to sharpen, as portions of the hosting matrix gradually undergo significant OH_2 loss allowing interaction of the dye with both tetra- and dihydrated sepiolite (and only the latter if temperature is further increased). As mentioned above, however, in spite of sepiolite partial (and reversible) dehydration due to loss of OH_2, no sharp evidence could be detected in our spectra, attesting to the existence of direct Mg/indigo interactions, often reported in previous works.[32,33,36,53]

3.2. Raman Spectroscopy. Raman spectra were collected in air on synthetic indigo and on the sepiolite + indigo (2 wt %) adduct after heating and Soxhlet extraction in $CHCl_3$ (Figure 6). The spectrum collected on a ground but unheated sepiolite + indigo mixture (not shown) proved to be basically identical to that of the heated sample, as Raman detectable clay/dye interactions begin to form and stabilize already during crushing, showing no appreciable (or just negligible) variation after heating.[39,68] Attempts to collect a Raman spectrum of pristine sepiolite brought no result, due to strong fluorescence effects already reported in previous papers.[69]

Collected spectra are consistent with previous literature data in spite of intensity variations affecting selected features, which may depend on the adopted excitation wavelength rather than on differences in the chemical surrounding. Assignment of Raman-active indigo modes (curve 1 in Figure 6) was based on the work of Tatsch and Schrader.[15]

All features appearing in the Raman spectrum of the sepiolite-based Maya Blue pigment are related to the indigo molecule, as the clay modes cannot be detected. The collected pattern is therefore basically consistent with others related to original Maya Blue specimens or palygorskite-based freshly synthesized analogues (in spite of their sometimes different indigo amounts),[20,35,64,68,70] contributions of different clays being hardly detectable.

Selected shifts and/or intensity fluctuations can be observed by comparing the spectra of indigo (curve 1 in Figure 6) and the related adduct with sepiolite (curve 2). Most significant differences can be summarized as follows: (i) A weak feature can be seen at 1731 cm^{-1} in the composite pattern (curve 2), which is absent in pure indigo. Such a band was never reported in the literature, although assignment to some combination mode cannot be excluded. (ii) The symmetric ν(C═O), coupled with ν(C═C) mode, significantly red-shifts passing from 1701 (indigo; curve 1) to 1687 cm^{-1} (sepiolite + indigo adduct; curve 2). Although a smaller shift (−7 cm^{-1}) was reported recently for an analogous sepiolite-based composite,[68] the magnitude observed here (−14 cm^{-1}) is consistent with those previously recorded for analogues hosted on palygorskite matrices.[20,64,70,71] The discussed evidence not only certifies the fundamental role played by the carbonyl group in host/guest interactions, but allows understanding of their nature: an equivalent shift, in fact, can be expected for a C═O involved in H-bonds with H_2O (−15 cm^{-1}, ab initio quantum methods[20]). Sharp consistency confirms that C═O acts as an acceptor of H-bonds from the nearest clay structural OH_2. (iii) Of the 1486−1464 cm^{-1} doublet of indigo [ν(C−C) coupled with C−H deformations] only the latter feature survives in the sepiolite-based composite (curve 2), while the component at higher wavenumbers disappears as observed in previous works.[20,64] (iv) Feature at 1365 cm^{-1} [δ(N−H) coupled with δ(C−H) modes] disappears almost completely in the sepiolite-based Maya Blue, implying that perturbations related to host/guest interactions also involve the N−H group of indigo. Although an analogous variation was reported previously,[64] it is exalted here by resonance effects.[20] (v) The 1224−1193 cm^{-1} doublet loses its lower-frequency feature in the sepiolite-based composite [ν(C−C) in rings] as a result of resonance due to reduced symmetry. (vi) Bands at 1632 [ν(C−C) in rings modes], 1590, and 1253 [δ(C−H), δ(C═O)] cm^{-1} show moderate intensity increase passing from indigo (curve 1) to Maya Blue (curve 2), implying activation of closely positioned Raman-inactive vibration modes of the B_u type.[68,70] Such behavior accounts for modifications and loss of planarity of the indigo molecule adsorbed in the microporous matrix. This phenomenon, already described for palygorskite-based analogues,[20] presumably accounts for the aforementioned partial oxidation of indigo to dehydroindigo.[26,72,73] Such a statement is reinforced as the observed enhancement of the 1632 cm^{-1} band can be also explained with the ν(C═N) typical of the dehydroindigo molecule.[74,75] Further evidence about the presence of dehydroindigo is given by the almost complete disappearance, in the composite pattern, of the weak indigo feature at 758 cm^{-1} sensitive to changes in the coordinative arrangement of the dye molecule.[76,77] (vii) At lower wavenumbers, intensity of the band related to δ(C−C) (674 cm^{-1}) significantly increases in Maya Blue (curve 2), presumably as the result of minor deformations, whereas bands at 601 and 549 cm^{-1} [mass dependent vibrations in five-membered rings: δ(C═O), δ(C−H), δ(C−NH−C) and δ(C═C−CO−C)] tend to broaden and decrease in intensity. Such variations, observed also by Vandenabeele et al.,[71] could imply combination of charge and symmetry effects[78] evidencing activation of Raman-forbidden modes due to the above-mentioned changes in planarity of the dye molecule. In agreement with other authors,[35,76,77] the peak at ≅ 601 cm^{-1} finds its correct attribution in the δ(C═C ring) of indigo (curve 1) rather than in straight cation/carbonyl (Al−O) interactions, sometimes suggested in the literature.[24] (vii) Observed intensity

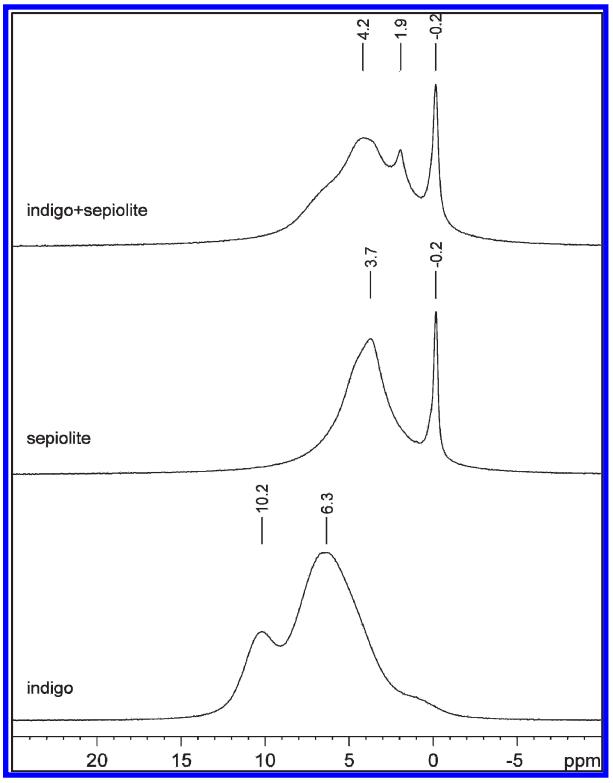

Figure 7. ^{1}H MAS NMR spectra of indigo, sepiolite, and sepiolite + indigo (2 wt %) Maya Blue recorded at 400.23 MHz with a spinning speed of 32 kHz.

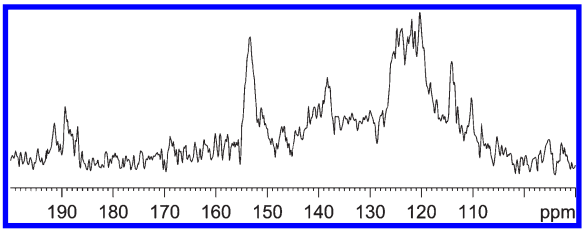

Figure 8. ^{13}C CPMAS NMR spectrum of sepiolite + indigo (2 wt %) Maya Blue recorded at 100.64 MHz with a spinning speed of 12 kHz.

Table 1. Assignment of ^{13}C NMR CPMAS Resonance Peaks of a Sepiolite-Based Maya Blue Pigment

sepiolite + indigo (2 wt %) (ppm)	indigo (ppm) (Doménech et al.[27])	assignment
191.4	188.5	3 (C═O)
189.3		
153.3	152.8	8 (C_q)
138.3	134.6	6 (CH)
signals around 122.2	124.5	2 (C_q)
	120.8	4 (CH) and 5 (CH)
114.1	113.5	9 (C_q) and 7 (CH)

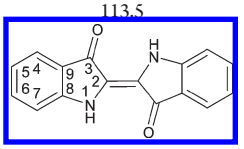

variations and/or shifts between pristine indigo and the sepiolite-based composite affecting Raman bands occurring at 549, 758, and 1576 cm^{-1} could be representative of changes in coordination of the indigo (or dehydroindigo) molecule. As these bands involve C═O and C═C bonds, such variations may also attest to the direct involvement of indigo carbonyl group in binding to the clay framework.[77]

3.3. Solid-State NMR Spectroscopy. ^{1}H NMR spectra were collected in air for pristine sepiolite, synthetic indigo, and the related heated and Soxhlet-extracted (2 wt %) composite (Figure 7).

Such technique is renowned for the detection and characterization of H-bonds,[79,80] as the presence of such interactions leads to a high-frequency shift of proton signals whose magnitude is related to the bond strength (as a rule, stronger H-bond interactions give higher chemical shift values[81,82]).

The ^{1}H NMR spectrum of solid-state indigo shows two broad resonances at 10.2 and 6.3 ppm, respectively: the former, less intense, is related to amine (N−H) groups; the latter is related to more abundant protons of the aromatic rings.

Two separate features appear in the spectrum of sepiolite: the broad signal at 3.7 ppm can be attributed to both zeolitic H_2O and structural OH_2 protons, whereas the sharp peak at −0.2 ppm is related to the framework hydroxyl groups coordinated by octahedral cations (Mg) in the TOT ribbons.

When sepiolite is ground and heated with 2 wt % indigo and Soxhlet extracted in $CHCl_3$, the related ^{1}H NMR spectrum preserves the narrow resonances at −0.2 ppm, which show no appreciable variation, whereas different signals occur at 1.9 and 4.2 ppm. While the former has to be reputed as an artifact attributed, with all due probability, to C−H leftovers of the Soxhlet solvent, the latter is due to small shifting of the clay peak related to H_2O and OH_2 protons. Such variation, already observed when palygorskite is the hosting matrix,[20] implies a slight modification of H_2O and OH_2 crystal−chemical surroundings due to the encapsulation of indigo within the sepiolite channels. The only evidence of indigo is a shoulder around 6.3 ppm, corresponding to non-shifted aromatic protons; the weak intensity of such signal is consistent with the low dye amount (2 wt %), which causes N−H proton peaks to be under the detection threshold.

Unfortunately, no measurable signal can be appreciated in the so-called strong H-bonding region (10−20 ppm), which is in agreement with previous results.[25] The observed evidence, however, does not necessarily imply total absence of H-bonds in the composite material: the lack of the related maxima, in fact, may indicate that in a sepiolite-based Maya Blue pigment the presumed host/guest interactions are weaker, both in strength and number, with respect to those existing in a palygorskite-based analogue, causing their detection to be under the threshold of the adopted technique. Additionally, possible uncovering of weaker H-bonds (typical of lower chemical shifts: 5−10 ppm) in the sepiolite + indigo (2 wt %) adduct appears to be even more troublesome by considering that such signals might be hidden beneath the more intense bands related to the hydrous clay content and indigo aromatic protons. On the contrary, in the palygorskite-based Maya Blue, features related to strong H-bonds (feeble resonance peaks at 17.8 and 13.0 ppm)[20] can be detected due to a lack of superposition with other more intense resonance peaks.

The ^{13}C CPMAS spectrum of the sepiolite + indigo (2 wt %) adduct is shown in Figure 8. The ^{13}C chemical shifts are listed in Table 1 together with those of pure indigo (as taken from Doménech et al.[27]).

In spite of its not so good signal/noise ratio (due to the very low indigo content), the comparison of the sepiolite + indigo ^{13}C CPMAS spectrum with that of previously reported compounds (i.e., pure indigo, indigo in palygoskite, and indigo in sepiolite[23,25,26]) allows some significant remarks. Indeed the small shifts observed, in particular those related to the carbonyl group resonance (3 C═O: from 188.5 to 191.4 ppm) and to peripheral C atoms of the aromatic rings (6 CH: from 134.6 to 138.3 ppm), are indicative of an intervened inclusion of the dye with the presence of weak interactions between the host and the guest.[83,84] The detected variations are consistent, although less evident, with those reported in previous works: most pronounced shifts, in fact, are known to appear at higher indigo content (11.5 wt %) and temperature (≥280 °C).[25] A lesser indigo amount (2 wt %) coupled with a less intense heating treatment (190 °C), which are consistent with those typical of the original Mayan artifact, therefore justifies the observed decrease in the magnitude of the detected variations. The observed trend is in agreement with the results of vibrational spectroscopies and with the lack of strong H-bonded signals in the ^{1}H MAS spectrum. The measured chemical shift is likely to be attributed to an indigo rather than dehydroindigo structure, according to the interpretation given by Doménech et al.[27] The presence of a small dehydroindigo amount under the limit of the instrumental detection due to scarce signal quality, however, cannot be ruled out: the quantity of dehydroindigo in Maya Blue, in fact, is always subordinated to that of indigo, being the related oxidation process far from completion.[23,26,27] On the other hand, the presence of many resonances around 122.2 ppm (attributed to the aromatic carbons) is consistent with the distortion of the molecule skeleton inside the hosting matrix, already evidenced by both IR and Raman results.

3.4. Structural Features of Sepiolite-Based Maya Blue. All collected experimental evidence allow postulation of a feasible structural model for the sepiolite-based Maya Blue, which includes an exhaustive description about the nature of the host/guest interactions responsible for the pigment stability.

FTIR data collected in real-time during synthesis of the sepiolite-based Maya Blue at progressively increasing temperatures in vacuum show the existence, for the hosting matrix, of two possible structural arrangements. By evacuating at 120 °C, almost all zeolitic H_2O is lost, while the total amount of structural OH_2 is still in the clay tunnels and superficial grooves (tetrahydrated sepiolite). Further heating at 150 °C in vacuum causes the additional loss of a significant fraction of the first half of Mg-coordinated OH_2, with consequent partial phase transformation from tetra- to dihydrated sepiolite. Structural folding typical of pristine dihydrated sepiolite, however, is inhibited by the intervened encapsulation of indigo within the clay tunnels: the presence of the dye molecule therefore severely modifies the structural features of the clay mineral, thus forming a completely new compound (unfolded dihydrated sepiolite + indigo) whose atypical behavior at increasing temperature is a straight consequence of the mutual host/guest interaction. In such a composite —which still contains a significant fraction (more than half) of Mg-coordinated OH_2, whose related stretching and bending modes remain clearly identifiable in the IR patterns—the crystallographic environment of the residual OH_2 molecules is varied with respect to pure sepiolite. Lack of structural folding due to indigo encapsulation, in fact, prevents interaction of the residual OH_2 molecules with the framework hydroxyls rendering them available to interact with the adsorbed dye by means of mutual H-bonds, whose existence is certified by perturbation of the related vibrational modes.

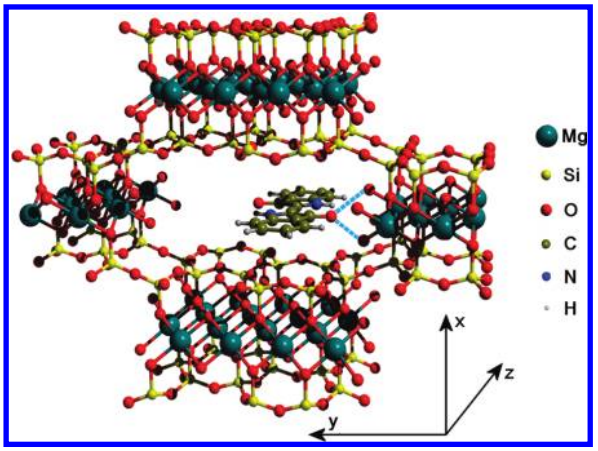

Figure 9. Host/guest interaction in sepiolite-based Maya Blue: the encapsulated indigo forms H-bonds (dashed lines) with Mg-coordinated OH_2 only on one side of its molecule, namely the one approaching the border of the sepiolite tunnel (zeolitic H_2O not shown for the sake of clarity).

Sorption on the hosting sepiolite framework causes crystalline indigo to fold as intermolecular bonds break, facilitating diffusion and encapsulation of isolated monomers within the wider clay channels (10.6 Å). Inclination for the sepiolite framework to shelter guest monomeric units inside its tunnels was also recently demonstrated for other dyes (Rhodamine 6G, Pyronine Y, and Styril 698 and 722).[38] Possible interaction of indigo aggregates with the clay surface, observed when different hosting matrices (i.e., zeolites) are involved,[29] is unlikely to happen, as no perturbation affects the superficial silanols nor can the existence of dye dimers be detected by means of UV−vis spectroscopy (absence of an absorption band at 680 nm).[29,39] Shifts and intensity fluctuations of selected vibrational modes prove that inside the channels of the hosting sepiolite matrix, emptied by preliminary loss of loosely bound zeolitic H_2O (necessary to favor indigo diffusion), a fraction of Mg-coordinated OH_2 is involved in interactions with the encapsulated guest dye molecules.

In an authentic (archeological) sepiolite-based Maya Blue, however, the encapsulated indigo molecules are expected to interact via H-bonds with a fully tetrahydrated hosting framework. IR spectra collected in air at room T on a freshly synthesized sepiolite-based Maya Blue (heated at 190° and Soxhlet extracted in $CHCl_3$) show relevant analogies, as far as indigo maxima are concerned, with those observed on the analogous composite heated at 120 °C in vacuum. In original Maya Blue, therefore, loss of structural OH_2 is not expected to happen or—if any—the related amount would be nonetheless replaced by consequent rehydration. The partial presence of dihydrated sepiolite (which requires higher temperatures to appear: ≥ 300 °C in air or ≥150 °C in vacuum), in fact, is not expected to significantly affect the nature of the host/guest interactions due to the reversibility of the semidehydration process (valid until temperature of 530 °C in vacuum is reached[48]).

The magnitude of the IR shifts related to sepiolite structural OH_2 modes is consistent with that expected for the establishment of H-bonding interactions. In spite of this, the corresponding intensities are sensibly weaker than those measurable when palygorskite is the hosting matrix.[64] This enhancement of the H-bond related signals noticeable in a palygorskite-based composite occurs even when lower indigo contents are fixated on the clay matrix (1 wt %).[20] In addition, the same tendency is confirmed by

combining the ^{1}H MAS and ^{13}C CPMAS solid-state NMR data, which is consistent with recent results attesting to the existence of H-bonds between coordinated OH_2 and indigo C═O/N−H groups in a sepiolite-based Maya Blue.[25]

The described differences affecting the intensities of the indigo-interacting OH_2 modes in palygorskite and sepiolite microporous matrices can be explained by taking into account the structural details of indigo accommodation in either clays. While in palygorskite indigo is juxtaposed in the middle of each channel[18,19] receiving H-bonds from coordinated OH_2 on both sides of the molecule, in the larger channels of sepiolite (10.6 Å) the dye monomers must get close to one border of the TOT ribbon in order to interact with the structural OH_2. By doing so, only one side of the molecule is H-bonded to the clay framework, whereas the other side—too far from the adjoining TOT border—may only weakly interact with the readsorbed zeolitic H_2O.[39] According to this model, indigo molecules are roughly oriented with their major dimension (≅12.3 Å) parallel to the tunnel axis (i.e., along z), lying approximately on the (100) crystallographic plane (Figure 9). Reliability of such a model was recently confirmed by theoretical assumptions obtained with computational modeling and experimentally checked by means of a crystal structure refinement using the Rietveld method on synchrotron powder diffraction data.[85] Alignment of the intercalated indigo molecules along the fiber elongation is consistent with the results recently obtained by Martìnez-Martìnez et al.,[38] who experimented on the possible sorption of different dyes in the same sepiolite hosting matrix.

As two indigo molecules cannot be paired side by side in a tunnel, the number of possible host/guest interactions in a sepiolite-based Maya Blue is potentially reduced (at least halved) with respect to a palygorskite-based one. The obvious consequence is that a palygorskite-based composite with indigo is sensibly more stable than its sepiolite-based analogue. Such structural features, coupled with the more enhanced fragility of the sepiolite framework, may contribute to weaken resistance to chemical attacks as performed stability tests seem to confirm.[37,86] This severe reduction in the global number of H-bonds justifies the modest intensities or chemical shifts (in IR and NMR patterns, respectively) of the related spectroscopic features compared to those typical of palygorskite-based analogues: in the sepiolite-based composite, in fact, an even smaller fraction of both coordinated OH_2 and dye reactive groups (C═O; N−H) is involved in the formation of host/guest interactions.

Similar perturbations affect both the carbonyl (C═O) and amine (N−H) groups of the encapsulated indigo, whose observed shifts show magnitudes that are also consistent with H-bonding formation in agreement with the dual nature (acceptor and donor) of the dye reactive groups. In addition to H-bonding with coordinated OH_2, both indigo groups may also interact with zeolitic H_2O readsorbed from environmental moisture once the composite is cooled to room temperature after synthesis.

Solvation on sepiolite causes deformation and loss of planarity of the indigo molecule, which may indirectly account for its partial oxidation to dehydroindigo. Such transformation could explain minor color changes observed during heating[28] and favor diffusion of the guest dye within the clay tunnels, as in dehydroindigo the rigid central C═C is substituted by a single C−C bond enhancing the molecule flexibility and ductility.[26,72,73]

No evidence was found about the existence of direct interactions between octahedral Mg and the carbonyl group of indigo, hypothesized by several authors,[22,32,36,87] although a limited interaction with Mg/Al ions (presumably superficial) acting as Lewis sites could be hypothesized for gaseous CO adsorbed on evacuated/activated sepiolite. Persistence at the adopted experimental conditions in the sepiolite framework of the whole (heating at 120 °C in vacuum or 190° in air) or more than half (150 °C in vacuum) Mg-coordinated OH_2 content and of intramolecular bonds in indigo possibly hinder straight C═O···Mg contact, thus preventing formation of this kind of interaction. Additionally, the thermal treatments applied in the current study were carefully selected in order to possibly respect the ancient procedures adopted by the Mayas themselves:[2] although sharp individuation of such parameters is still open to discussion, it is generally acknowledged that moderate temperatures (between 120 and 200 °C in air) are more than sufficient to justify the synthesis of a clay/indigo composite analogous to original Maya Blue.[3,4,35,37,88,89] In spite of this, it is legitimate to repute that exposure to higher temperatures (≥300 °C) could favor the formation of different kinds of host/guest interactions, i.e., direct Mg−indigo interactions, as previous works pointed out.[23,36] Recent experiences, however, showed that these straight interactions between octahedral ions and carbonyl/ammine groups of indigo tend to disappear in time, as the high-temperature clay/dye composites are cooled in a moisturizing environment.[53]

4. CONCLUSIONS

A freshly synthesized sepiolite-based Maya Blue pigment was studied by means of FTIR, Raman, and NMR spectroscopies with the aim to characterize both the site and nature of the interactions occurring between the hosting clay matrix and the guest indigo molecule, responsible for the compound stability.

Collected evidence unequivocally proved that host/guest interactions are likely to form between the tightly bound Mg-coordinated OH_2 of sepiolite and the acceptor and donor groups (C═O and N−H) of indigo, whose related signals undergo perturbation due to their mutual interaction evidencing magnitudes consistent with the hydrogen nature of such bonds.

Formation of H-bonds is independent from the level of hydration of the hosting matrix, as their existence can be detected either in the tetrahydrated (full structural OH_2 content) or in the dihydrated (loss of almost first half of OH_2) sepiolite + indigo (2 wt %) composite, assuming that the weakly bound zeolitic H_2O is lost during heating.

The presence of indigo inhibits structural folding, which occurs in pristine dihydrated sepiolite after loss of the first half of Mg-coordinated OH_2. Encapsulation of the guest molecule therefore allows, if temperature is above a prefixed threshold (≥300 °C in air or 150 °C in vacuum), the existence of an atypical structural arrangement formed by an unfolded dihydrated sepiolite matrix, which hosts and shelters the guest indigo molecules in its noncollapsed internal channels (10.6 × 3.7 Å). Lack of folding implies variation of the crystallographic environment for the residual OH_2 molecules, which become available for H-bonding formation with the dye reactive groups.

Encapsulation of indigo is favored by breaking of intermolecular bonds among different dye molecules, which allows diffusion of single monomers and bonding within the sepiolite channels. A limited indigo fraction is likely to undergo oxidation to dehydroindigo, whose enhanced flexibility implies loss of planarity and molecule deformation.

The encapsulated indigo monomers can form H-bonds only on one side of the molecule, namely, the one approaching the tunnel border. As a result, the global number of possible H-bonds

existing in sepiolite-based Maya Blue is dramatically reduced with respect to a palygorskite-based one, where indigo can interact with both sides of the narrower channels. Such peculiarity affects the stability of the resulting compound, thus justifying the renowned intrinsic fragility of sepiolite-based Maya Blue when compared to its palygorskite-based counterpart.

No straight evidence was found on the existence of direct interactions between octahedral Mg ions and the carbonyl group of indigo, which is consistent with the adopted thermal treatment being comparable to those used by the ancient Mayas themselves. Adoption of more severe heating conditions (i.e., ≥ 300 °C in air), however, might originate different kinds of host/guest interaction.

AUTHOR INFORMATION

Corresponding Author

*E-mail: roberto.giustetto@unito.it.

ACKNOWLEDGMENT

The authors wish to thank Prof. Giacomo Chiari, who first drove them inside the crowded microtunnels of Maya Blue pigment. We would like to thank the referees of this paper (anonymous) who helped with their hints, suggestions, and comments to significantly improve the manuscript quality. Special thanks go to Prof. Giovanni Ferraris for his valuable advice and support.

REFERENCES

(1) Merwin, H. E. Carnegie Institution of Washington Publication 406, Washington D.C., 1931.
(2) Reyes-Valerio, C. De Bonampak al Templo Mayor: el Azul Maya en Mesoamerica, Siglo XXI Ed.es, Mexico, 1993.
(3) Van Olphen, H. *Science* **1966**, *154*, 645–646.
(4) Kleber, R.; Masschelein-Kleiner, L.; Thissen, J. *Studies in Conservation* **1967**, *12*, 41–55.
(5) Ferraris, G.; Makovicky, E.; Merlino, S. *Crystallography of Modular Materials*; IUCr/Oxford University Press: Oxford, 2004.
(6) Bailey, S. W.; Alietti, A.; Brindley, G. W.; Formosa, M. L. L.; Jasmund, K.; Konta, J.; Mackenzie, R. C.; Nagasawa, K.; Rausell-Colom, R. A.; Zvyagin, B. B. *Clays Clay Miner.* **1980**, *28* (1), 73–78.
(7) Akyuz, S.; Akyuz, T.; Davies, J. E. D. *J. Mol. Struct.* **1993**, 279.
(8) Akyuz, S.; Akyuz, T.; Davies, J. E. D.; Esmer, K.; Ozel, E. J. *Raman Spectrosc.* **1995**, 883.
(9) Shariatmadari, H; Mermut, R.; Benke, M. B. *Clays Clay Miner.* **1999**, *47*, 44–53.
(10) Özdemir, Y; Dogan, M.; Alkan, M. *Microporous Mesoporous Mater.* **2006**, *96*, 419–427.
(11) Bilgiç, C *J. Colloid Interface Sci.* **2005**, *281*, 33–38.
(12) Occelli, M. L.; Maxwell, R. S.; Eckert, H. *J. Catal.* **1992**, *137*, 36–50.
(13) Suarez, S.; Coronado, J. M.; Portela, R.; Carlos Martin, J.; Yates, M.; Avila, P.; Sanchez, B. *Environ. Sci. Technol.* **2008**, *42* (16), 5892–5896.
(14) Kong, Y.; Chen, X. H.; Ni, J. H.; Yao, S. P.; Wang, W. C.; Luo, Z. Y.; Chen, Z. D. *Appl. Clay Sci.* **2010**, *49*, 64–68.
(15) Tatsch, E.; Schrader, B. *J. Raman Spectrosc.* **1995**, *26*, 467–473.
(16) Klessinger, M.; Lüttke, W. *Chem. Ber.* **1966**, *99*, 2136–45.
(17) Yasarawan, N.; Van Duijneveldt, J. S. *Langmuir* **2008**, *24*, 7184–7192.
(18) Giustetto, R.; Levy, D.; Chiari, G. *Eur. J. Miner.* **2006**, *18*, 629–640.
(19) Chiari, G.; Giustetto, R.; Ricchiardi, G. *Eur. J. Miner.* **2003**, *15*, 21–33.
(20) Giustetto, R.; Llabres I Xamena, F.; Ricchiardi, G.; Bordiga, S.; Damin, A.; Chierotti, M. R.; Gobetto, R. *J. Phys. Chem. B* **2005**, *109* (41), 19360–19368.
(21) Chiari, G.; Giustetto, R.; Druzik, J.; Dohene, E.; Ricchiardi, G. *Appl. Phys. A: Mater. Sci. Process.* **2008**, *90*, 3–7.
(22) Polette-Niewold, L. A.; Manciu, F. S.; Torres, B.; Alvarado, M., Jr; Chianelli, R. R. *J. Inorg. Biochem.* **2007**, *101*, 1958–1973.
(23) Ovarlez, S.; Giulieri, F.; Chaze, A. M.; Delamare, F.; Raya, J.; Hirschinger, J. *Chem.—Eur. J.* **2009**, *15*, 11326–11332.
(24) Manciu, F. S.; Reza, L.; Polette, L. A.; Torres, B.; Chianelli, R. R. *J. Raman Spectrosc.* **2007**, *38*, 1193–1198.
(25) Raya, J.; Hirschinger, J.; Ovarlez, S.; Giulieri, F.; Chaze, A. M.; Delamare, F. *Phys. Chem. Chem. Phys.* **2010**, DOI: 10.1039/c0cp00834f.
(26) Doménech, A.; Doménech-Carbò, M. T.; Sànchez del Rio, M.; Vazquez de Agredos Pascual, M. L.; Lima, E. *New J. Chem.* **2009**, *33*, 2371–2379.
(27) Doménech, A.; Doménech-Carbò, M. T.; Sànchez del Rio, M.; Goberna, S.; Lima, E. *J. Phys. Chem. C* **2009**, *113* (28), 12118–12131.
(28) Rondão, R.; Seixas de Melo, S.; Bonifácio, V. D. B.; Melo, M. J. *J. Phys. Chem. A* **2010**, *114*, 1699–1708.
(29) Dejoye, C.; Martinetto, P.; Dooryhée, E.; Strobel, P.; Blanc, S.; Bordat, P.; Brown, R.; Porcher, F.; Sanchez del Rio, M.; Anne, M. *Appl. Mater. Interfaces* **2010**, *8*, 2308–2316.
(30) Fois, E.; Gamba, A.; Tilocca, A. *Microporous Mesoporous Mater.* **2003**, *57*, 263–272.
(31) Reinen, D.; Köhl, P.; Muller, C. *Z. Anorg. Allg. Chem.* **2004**, *630*, 97–103.
(32) Manciu, F. S.; Ramirez, A.; Durrer, W.; Govani, J.; Chianelli, R. R. *J. Raman Spectrosc.* **2008**, *39*, 1257–1261.
(33) Tilocca, A.; Fois, E. *J. Phys. Chem. C* **2009**, *113*, 8683–8687.
(34) Hubbard, B.; Wenxing, K.; Moser, A.; Facey, G. A.; Detellier, C. *Clays Clay Miner.* **2003**, *51* (3), 318–326.
(35) Sànchez Del Rio, M.; Boccaleri, E.; Milanesio, M.; Croce, G.; Van Beek, W.; Tsiantos, C.; Chryssikos., G. D.; Gionis, V.; Kacandes, G. H.; Suarez, M.; Garcia-Romero, E. *J. Mater. Sci.* **2009**, *44*, 5524–5536.
(36) Ovarlez, S.; Chaze, A. M.; Giulieri, F.; Delamare, F. *C. R. Chim.* **2006**, *9*, 1243–1248.
(37) Sànchez Del Rio, M.; Martinetto, P.; Reyes-Valerio, C.; Dooryhée, E.; Suárez, M. *Archaeometry* **2006**, *48* (1), 115–130.
(38) Martìnez-Martìnez, V; Corcóstegui, C.; Bañuelos Prieto, J.; Gartzia, L.; Salleres, S.; López Arbeloa, I. *J. Mater. Chem.* **2011**, *21*, 269–276.
(39) Giustetto, R.; Seenivasan, K.; Bordiga, S. *Period. Mineral.* **2010**, *79*, 21–37.
(40) Nakanaga, T.; Buchold, K.; Ito, F. *Chem. Phys.* **2003**, *288*, 69–76.
(41) Garcia-Viloca, M.; Gelabert, R.; Gonzalez-Lafont, A.; Moreno, M.; Lluch, J. M. *J. Phys. Chem. A* **1997**, *101*, 8727–8733.
(42) Farmer, V. C., Ed. *The Infrared Spectra of Minerals*; Mineralogy Society: London, 1974.
(43) Frost, R. L.; Locos, O. B.; Ruan, H.; Kloprogge, J. T. *Vib. Spectrosc.* **2001**, *27*, 1–13.
(44) Jung, S. M.; Grange, P. *Appl. Surf. Sci.* **2004**, *221*, 167–177.
(45) Hayashi, H.; Otsuka, R.; Imai, N. *Am. Mineral.* **1969**, *53*, 1613–1624.
(46) Cannings, F. R. *J. Phys. Chem.* **1968**, *72*, 1072–1074.
(47) Angell, C. L.; Schaffer, P. C. *J. Phys. Chem.* **1965**, 3463.
(48) Serna, C.; Ahlrichs, J. L.; Serratosa, J. M. *Clays Clay Miner.* **1975**, *23*, 452–457.
(49) Nagata, H.; Shimoda, S.; Sudo, T. *Clays Clay Miner.* **1974**, *22*, 285–293.
(50) Post, J. E.; Bish, D. L.; Heaney, P. J. *Am. Mineral.* **2007**, *92*, 91–97.
(51) Lokanatha, S.; Mathur, B. K.; Samantaray, B. K.; Bhattacherjee, S. *Z. Kristallogr.* **1985**, *171*, 69–79.
(52) Preisinger, A. *Clays Clay Miner.* **1963**, *10*, 365–371.
(53) Ovarlez, S.; Giulieri, F.; Delamare, F.; Sbirrazzuoli, N.; Chaze, A. M. *Microporous Mesoporous Mater.* **2011**, DOI: 10.1016/j.micromeso.2010.12.025.

(54) Mendelovici, E. *Clays Clay Miner.* **1973**, *21*, 115.
(55) Prost, R. *Spectrochim. Acta* **1975**, *31A*, 1497.
(56) Mendelovici, E.; Portillo, D. C. *Clays Clay Miner.* **1976**, *24*, 177.
(57) Ahlrichs, J. L.; Serna, C.; Serratosa, J. M. *Clays Clay Miner.* **1975**, *23*, 119.
(58) Van Der Marel, H. W.; Beutelspacher, H. *Atlas of Infrared Spectroscopy of Clay Minerals and Their Admixtures*; Elsevier: Amsterdam, 1976.
(59) Zecchina, A.; Otero Arean, C. *Chem. Soc. Rev.* **1996**, *25* (3), 187–197.
(60) Zecchina, A.; Spoto, G.; Bordiga, S. *Phys. Chem. Chem. Phys.* **2005**, *7*, 1627–1642.
(61) Weinstein, J.; Wyman, G. M. *J. Am. Chem. Soc.* **1956**, *78*, 2387.
(62) Süsse, P.; Steins, M.; Kupcik, V. *Z. Kristallogr.* **1988**, *184*, 269–273.
(63) Kuang, W.; Facey, G. A.; Detellier, C.; Casal, B.; Serratosa, J. M.; Ruiz-Hitzky, E. *Chem. Mater.* **2003**, *15*, 4956–4967.
(64) Leona, M.; Casadio, F.; Bacci, M.; Picollo, M. *J. Am. Inst. Conserv.* **2004**, *43* (1), 39–54.
(65) Kuang, W.; Facey, G. A.; Detellier, C. *J. Mater. Chem.* **2006**, *16*, 179–185.
(66) Kitayama, Y.; Kamimura, M.; Wakui, K.; Kanamori, M.; Kodama, T.; Abe, J. *J. Mol. Catal. A: Chem.* **1999**, *142*, 237–245.
(67) Klessinger, M.; Luettke, W. *Tetrahedron Lett.* **1963**, *19* (2), 315.
(68) Sànchez del Rio, M.; Picquart, M.; Haro-Poniatowski, E.; Van Elslande, E.; Hugo, Uc V. *J. Raman Spectrosc.* **2006**, *37*, 1046–1053.
(69) McKeown, D. A.; Post, J. E.; Etz, E. S. *Clays Clay Miner.* **2002**, *5*, 667–680.
(70) Witke, K.; Brzezinka, K. W.; Lamprecht, I. *J. Mol. Struct.* **2003**, *661−662*, 235–238.
(71) Vandenabeele, P.; Bodé, S.; Alonso, A.; Moens, L. *Spectrochim. Acta, Part A* **2005**, *61*, 2349–2356.
(72) Doménech, A.; Doménech-Carbò, M. T.; Vàsquez de Agredos Pascual, M. L. *J. Phys. Chem. B* **2006**, *110*, 6027–6039.
(73) Doménech, A.; Doménech-Carbò, M. T.; Vàsquez de Agredos Pascual, M. L. *J. Phys. Chem. C* **2007**, *111*, 4585–4595.
(74) Jeon, S.; Woo, J.; Kyong, J. B.; Choo, J. *Bull. Korean Chem. Soc.* **2001**, *22*, 1264.
(75) Bruneel, J. L.; Lassegues, J. C.; Sourisseau, C. J. *Raman Spectrosc.* **2002**, *33*, 815.
(76) Tomkinson, J.; Bacci, M.; Picollo, M.; Colognesi, D. *Vib. Spectrosc.* **2009**, *50*, 268.
(77) Doménech, A.; Doménech-Carbò, M. T.; Edwards, H. G. M. *J. Raman Spectrosc.* **2011**, *42*, 86–96.
(78) Coupry, C.; Sagon, G.; Gorguet-Ballesteros, P. *J. Raman Spectrosc.* **1997**, *28*, 85–89.
(79) Chierotti, M. R.; Gobetto, R. *Chem. Commun.* **2008**, 1621–1634.
(80) Chierotti, M. R.; Ferrero, L.; Garino, N.; Gobetto, R.; Pellegrino, L.; Braga, D.; Grepioni, F.; Maini, L. *Chem.—Eur. J.* **2010**, *16*, 4347–4358.
(81) Sternberg, U.; Brunner, E. *J. Magn. Reson, Ser. A* **1994**, *108*, 142.
(82) Frey, P. A. *Magn. Reson. Chem.* **2001**, *39*, S190–S198.
(83) Chierotti, M. R.; Gobetto, R. *Eur. J. Inorg. Chem.* **2009**, 2581–2597.
(84) Aime, S.; Chierotti, M. R.; Gobetto, R.; Masic, A.; Napolitano, F.; Canuto, H. C.; Heyes, S. J. *Eur. J. Inorg. Chem.* **2008**, 152–157.
(85) Giustetto, R.; Levy, D.; Wahyudi, O.; Ricchiardi, G.; Vitillo, J. G. *Eur. J. Mineral.* **2011**, *23*, 449–466.
(86) Giustetto, R.; Wahyudi, O.; Corazzari, I.; Turci, F. *Appl. Clay Sci.* **2011**, *52*, 41–50.
(87) Fuentes, M. E.; Peña, B.; Contreras, C.; Montero, A. L.; Chianelli, R.; Alvarado, M.; Olivas, R.; Rodrìguez, L. M.; Camacho, H.; Montero-Cabrera, L. A. *Int. J. Quantum Chem.* **2008**, *108* (10), 1664–1673.
(88) Littmann, E. R. *Am. Antiq.* **1982**, *47*, 404–408.
(89) Torres, L. *Mater. Res. Soc. Symp. Proc.* **1988**, *123*, 123–128.